Controllable elastocapillary folding of silicon nitride 3D structures by through-wafer filling

A. Legrain*, T.G. Janson, J.W. Berenschot, G.J.M. Krijnen, L. Abelmann and N.R. Tas
MESA+ Institute for Nanotechnology, University of Twente, The Netherlands
*Corresponding author: Antoine Legrain, a.b.h.legrain@utwente.nl

***Abstract*—We present the controllable capillary folding of planar silicon nitride templates into 3D micro-structures by means of through-wafer liquid application. We demonstrate for the first time hydro-mechanical, repeatable, actuation of capillary folded structures via addition or retraction of water on demand.**

I. Introduction

A. Elastocapillary folding

Elastocapillary phenomena refer to the deformation of objects due to capillary effects of liquid droplets or films [1]. The final deformation is governed by the balance between bending and capillary forces. It is helpful to define an elastocapillary length, $L_{ec} = (B/\gamma)^{1/2}$ where B is the bending stiffness [N/rad] and γ the surface tension [Nm^{-2}]. Typically, objects larger than the elastocapillary length are significantly deformed by capillary forces [2].

Previously, we have combined elastocapillary interactions with micro-machining to fabricate 3D silicon nitride micro-objects, starting from flat patterns – a method we called elastocapillary folding or capillary origami [3], [4]. This more deterministic form of self-assembly of 3D objects enabled by a weak interaction (here, surface tension) can be generally defined as self-folding [5].

A 2D elastocapillary model has been developed and we showed that this simplistic model can be used to accurately describe the self-folding of 2D extruded prismatic structures. The outcome of the folding (closed or reopened) is determined by a parameter which is closely related to the elastocapillary length [3].

The continuous demand for smaller functional elements in microtechnology brings the necessity to use all three spatial dimensions effectively. By combining the assets of mask-based fabrication and self-assembly, self-folding is a promising approach to reach the third dimension.

B. Hydromechanical actuation

In our previous works on elastocapillary folding we manually deposited a droplet on the structures [3], [4]. This technique suffers from several disadvantages, such as difficult droplet application and lack of control of applied volume. Moreover, the structures can be folded only once, which considerably limits their potential applications.

Although the actuation of self-folded structures by pH triggering or temperature variation has been reported (see for instance the review by Leong *et al.* [5]), not much work has been done on elastocapillary folded structures [1]. On the macro-scale, elegant control of folding by an electric field has been demonstrated [6], [7], but this method is difficult to apply to micrometer structures in which the integration of electrodes and the control of small volume of water remain complicated.

In this paper, we present the first demonstration of folding by through-wafer filling. This technique, presented in Fig. 1, enables three-dimensional hydro-mechanical actuation of micro-structures. Along with the technical details on fabrication and experiments, an analytical study of the folding process is presented.

II. Theory

The theory developed for elastocapillary folding by front size droplet application [3] has to be extended for back-side filling. When the meniscus proceeding through the tube meets the diverging section at the top of the tube, it is pinned. The overpressure needed to overcome the pinning effect and to advance the meniscus on top of the origami pattern is given by the Young-Laplace equation:

$$\Delta P_{\text{max}} = -\frac{4\gamma\cos\left(\theta_{\text{a}} + \frac{\pi}{2}\right)}{D_0}$$

where γ is the surface tension of water, θ_{a} the advancing contact angle of water on silicon nitride and D_0 the maximum diameter of the tube [8]. In case of a practical fluidic system, which is not infinitely stiff, this overpressure causes a slight

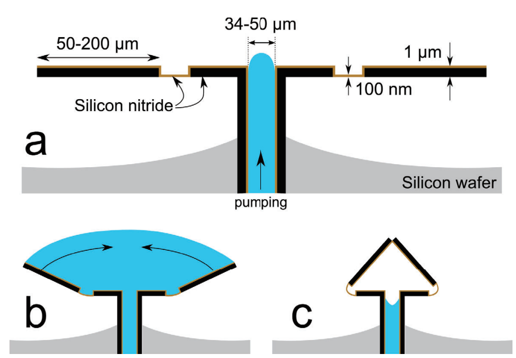

Fig. 1. Sketch of folding principle. (a) Water is pumped through the wafer via the central tube. The liquid flows over the silicon nitride structure and pumping is stopped. (b) The water tends to reduce its liquid-air interface and provokes the rotation of the flaps through the bending of the thin hinges. The volume of liquid either decreases by evaporation or by deliberate retraction. (c) Once the water is gone, the flaps adhere together.

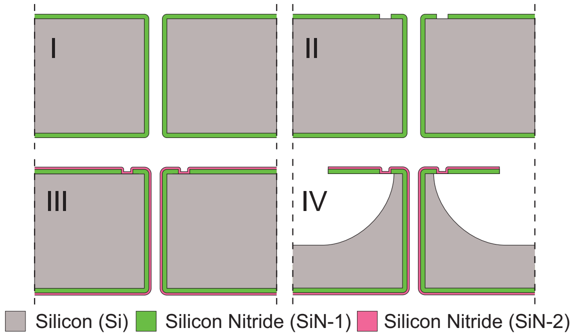

Fig. 2. Fabrication outline. I: A tube is drilled all through the wafer using a DRIE Bosch process. A 1 µm thick layer of silicon nitride (SiN-1) is conformally deposited. II: The layer SiN-1 is dry etched in a plasma system after a second lithographic step. III: A second 100 nm thin layer is deposited (SiN-2). This layer is thin enough to be deformed by surface tension. IV: A final lithographic step is used to define the overall geometry of the structures and to release them by a semi-isotropic SF_6 silicon etch.

increase of the total amount of liquid in the system. Once the meniscus leaves the tube, the overpressure reduces which releases additional liquid from the system resulting in an overshoot.

III. Experimental

A. Fabrication

Fig. 2 shows a concise outline of the fabrication process for the origami patterns used in the experiments. Fig. 3 shows the resulting structure. The three lithographic steps following the drilling of the tubes were performed using spray resist for an optimal protection of the edges of the tubes. Low stress silicon-rich nitride layers were deposited by LPCVD. The structures were cleaned in HNO_3 just before the last lithographic step and final cleaning is done by oxygen plasma.

B. Fluidic setup

A schematic of the fluidic setup is shown in Fig. 4. The elasticity of the system was designed to be as small as possible

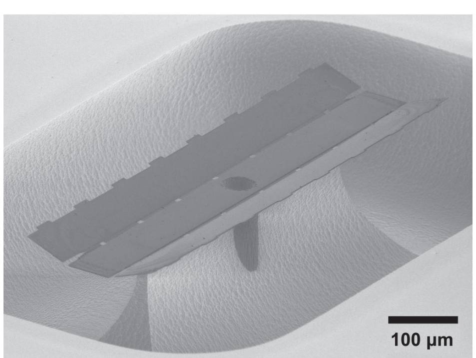

Fig. 3. SEM image of a silicon nitride origami template with two flaps, resting on a silicon pillar with a hollow silicon nitride tube. Length of the structure is 800 µm and flap width is 80 µm. The hinges are 7 µm wide and diameter of the tube is 50 µm. Holes were patterned along the hinges to reduce their stiffness. Note that the flaps are not initially aligned with the central part. This type of structure was used for the analysis presented in Fig. 6 and 8.

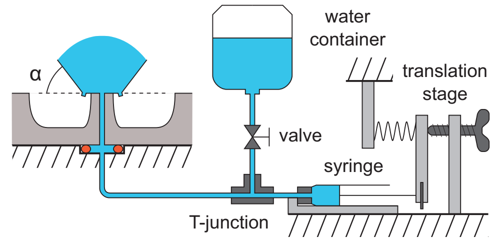

Fig. 4. Schematic of fluidic setup filled with ultra clean water. Fluidic connection to the wafer is made with a recessed o-ring in a metal part. Tubing is thick-walled (PEEK) and the syringe is made of glass. The angle α represents the rotation of the flaps, plotted in Fig. 6 and 8.

to limit the amount of overshoot. Fluidic connection to the tube in the wafer is achieved by a tiny recessed o-ring in a metal part. The wafer sits on the metal part and the connecting force is predominantly transferred between metal and wafer. In this way we aim to limit the change in compression of the o-ring under liquid pressure variation. Other measures are the use of a Hamilton glass syringe and thick-walled PEEK tubing. Finally, the volume between the syringe plunger and the sample is kept as low as possible (around 10 µL).

IV. Results

A. Overshoot

To quantify the overshoot of the fluidic setup the syringe pump was quasi-statically actuated, starting with water in the through-wafer tube filled by capillarity. When water exceeded the edge of the tube and wetted the surface, actuation of the pump was stopped. The water droplet volume was derived from snapshots of the captured video. Measurements on geometrical features of identical structures in SEM images were used as reference. Fig. 5 shows the snapshots that were used to determine the volumes. The left part shows the typical excess volume before revision of the fluidic set-up, which translates to 93 ± 12 nL. The error is due to the uncertainty in identifying the features of the droplets in the images. After improving the setup (right part of Fig. 5), the overshoot reduced to 1.4 ± 0.4 nL. However, the tube diameter in the first case is 34 µm, versus 50 µm in the second. After taking the overpressure

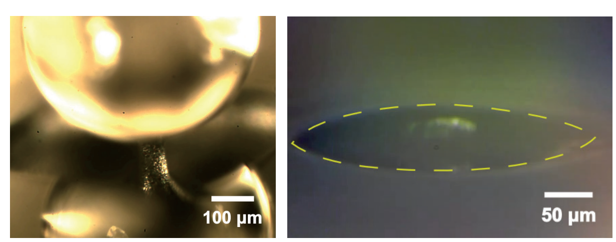

(a) (b)

Fig. 5. Comparison of the amount of excess of liquid before (left) and after (right) the optimization of the set-up. The yellow dashed line in the right hand picture denotes the contour of the drop; the height at the center the drop is approximately 40 µm. This drop is resting on a large silicon nitride platform that cannot be seen here. By selecting rigid components and decreasing the internal volume, the overshoot was reduced by approximately a factor 50.

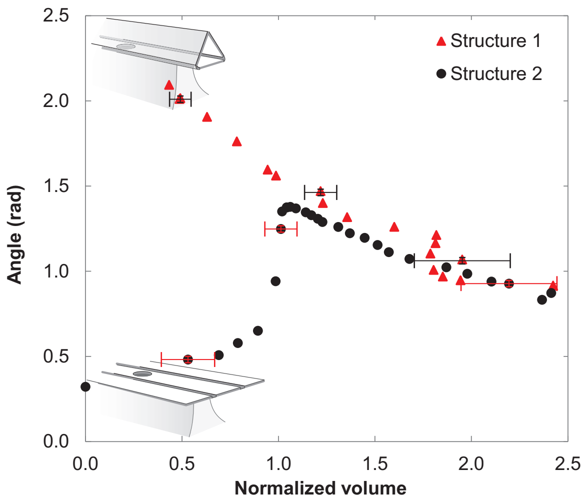

Fig. 6. Flap angle α versus liquid volume, for two structures similar to those shown in Fig. 3) but with a difference in spring constant. Structure 1 (red triangles) closes completely. The stiffer structure 2 (black circles) does not attain the maximal rotation and reopens.

difference into account, this results in a reduction of the overshoot volume by an approximate factor 50.

B. Elastocapillary folding

We realized two structures with different length of perforation in the hinges (see Fig. 3). The hinges in structure 1 are 50 % longer than in structure 2, resulting in a difference in stiffness of 50 %.

The evolution of folding of 2D extruded prismatic structures (Fig. 3) was recorded during the evaporation of water after the structures had been wetted by through-wafer filling. The angle of rotation of the flaps with respect to the central part (see Fig. 4) was extracted, along with the normalized volume of water: the surface of water from the side view normalized by $\frac{1}{w^2}$, where w is the width of the flaps [3].

Fig. 6 shows that structure 1 folds until reaching the maximum folding angle, $\alpha_{max} = \frac{2\pi}{3}$, at which the object will stay closed because of sufficiently large stiction forces.

On the other hand, the stiffer structure 2 does not attain the maximal angle of rotation during folding. While the volume decreases due to the evaporation of water, the surface energy decreases and, at a certain point, cannot sustain the increasing bending energy anymore. The structure then reopens and the flaps come back to their initial position. This difference in behavior is in agreement with the theory and results presented in our previous work [3].

C. Repeatable folding

The novelty of this through-wafer filling technique is the possibility to repeatedly open and close the structures. Fig. 7 shows the actuation of a cubic structure. Once the pinning of water at the edge of the tube is overcome, accurate addition and retraction of water is possible by using the syringe pump. Controlled reopening of structures was impossible using the top filling method that we employed in our previous work [3], [4]. Our structures were actuated up to 20 times without showing any signs of wear. However, endurance experiments to test the long-term stability have not been carried out yet.

The folding of structures, which takes a few minutes when letting the water evaporate (Fig. 7 between b and d), can be considerably sped up to times less than a second by retracting water through the tube. Furthermore, by tuning the height of the water container (see Fig. 4) it is possible to set the applied pressure and ”freeze” the folding structure for certain ranges of states. This situation evidently implies that water is added to compensate for the evaporation.

Surprisingly, a structure that undergoes several actuations shows a different behavior for every iteration, as shown in Fig.8. While the flaps reach an angle of 80^o before reopening during the first actuation, the maximal angle of rotation drops to 40^o during the fifth iteration. Two parameters could explain this behavior: a change in stiffness of the hinges and a drop of surface tension through the actuation cycles.

D. Residues on the structures

Large amounts of residue were observed on the structures after their actuation, see Fig. 9. This residue seems to aggregate at the level of the hinges during repeated folding. The residue is probably caused by the fabrication process, which contains a final release step that cannot be followed by a liquid cleaning step (see Fig. 2).

Whether these residues are diluted in the water during folding or stay on the hinges is not clear yet. Both situations explain the results presented in the previous section, however. Residues deposited on the hinges make them thicker and therefore stiffer, whereas the surface tension of water can possibly drop when polluted.

V. Discussion

Our novel backside-filling elastocapillary folding method allows repeated assembly of 3D micro-structures, which has to our knowledge never been demonstrated before. Our optimized setup allow us to actuate these 3D objects in a well-controlled way. However, the fact that the structures become polluted during the actuation is a major drawback. We believe residue causes both the structure and the water to change. This makes a comparison to the existing model, presented in [3], impossible. While the folding curves look similar to theory, we cannot draw any conclusions. Further work on this subject will therefore focus on avoiding the residue and extending the analytical study of the folding behavior.

VI. Conclusion

We demonstrated controllable capillary folding of planar silicon nitride templates into 3D micro-structures by means of through-wafer liquid application. For the first time, hydromechanical, repeatable actuation of capillary folded structures via subsequent addition and retraction of water has been achieved.

Through-wafer filling requires a sufficiently high pressure to overcome pinning of the liquid meniscus at the edge of the

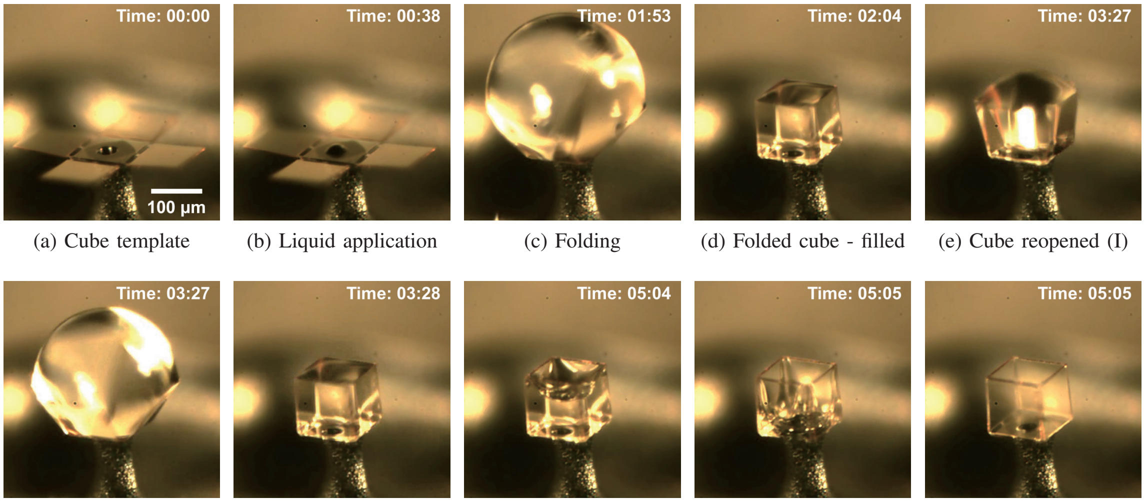

(a) Cube template (b) Liquid application (c) Folding (d) Folded cube - filled (e) Cube reopened (I)

(f) Cube reopened (II) (g) Cube closed (h) Liquid retraction (I) (i) Liquid retraction (II) (j) Folded cube - empty

Fig. 7. (a-h). Chronological sequence of snapshots from a movie of the folding process of a five-faced cube with rib length of 100 µm (Time format: mm:ss). Between b) and d) the folding occurred by allowing the water to evaporate. In the time between d) and h), the cube was repeatedly opened and closed (20 times). One sequence of opening and closing is shown from e) to g).

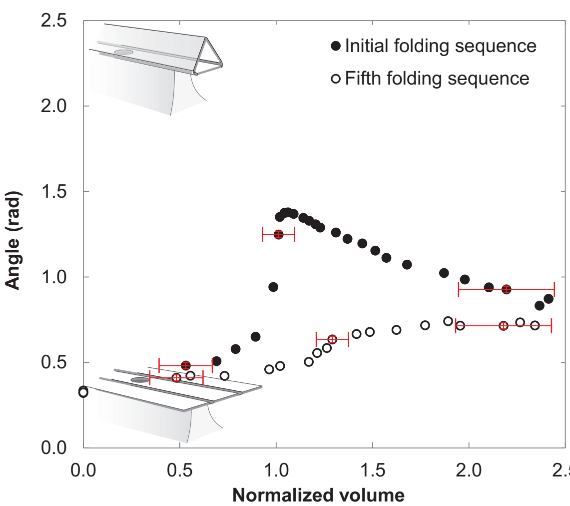

Fig. 8. Flap angle versus volume for the same structure measured for the first folding sequence (closed circles) and during the fifth sequence (open circles). The maximal rotation angle decreases with the number of iterations.

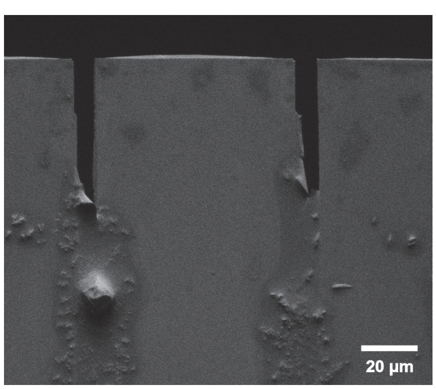

Fig. 9. SEM picture of the top part of the silicon nitride template after several folding sequences, showing the accumulation of residue on the hinges.

tube. This high pressure in combination with the elasticity of the fluidic set-up causes an overflow of water. Precise hydro-mechanical actuation can only be achieved by selecting rigid components for the fluidic setup. In our situation, the volume of excess liquid could be reduced to 1.4 ± 0.4 nL.

Folding of a structure that does not fully close was monitored during five repeated cycles of filling and subsequent evaporation of water. The maximum folding angle decreased with every cycle.

Our results demonstrate that multiple elastocapillary folding in the micrometer scale is possible, which opens a route towards more complex structures, micro-actuation and possibly drug delivery.

References

[1] J.-L. Liu and X.-Q. Feng, "On elastocapillarity: A review," *Acta Mechanica Sinica*, vol. 28, pp. 928–940, 2012. [Online]. Available: http://dx.doi.org/10.1007/s10409-012-0131-6

[2] C. Py, P. Reverdy, L. Doppler, J. Bico, B. Roman, and C. N. Baroud, "Capillary origami: Spontaneous wrapping of a droplet with an elastic sheet," *Phys Rev Lett*, vol. 98, no. 15, p. 156103, 2007.

[3] J. W. van Honschoten, T. Berenschot, J. W. Ondarçuhu, R. G. P. Sanders, J. Sundaram, M. Elwenspoek, and N. R. Tas, "Elastocapillary fabrication of three-dimensional microstructures," *Appl. Phys. Lett.*, vol. 97, pp. 0 141 031–0 141 033, 2010.

[4] J. van Honschoten, A. Legrain, J. Berenschot, L. Abelmann, and N. Tas, "Micro-assembly of three dimensional tetrahedra by capillary forces," in *Micro Electro Mechanical Systems (MEMS), 2011 IEEE 24th International Conference on*, jan. 2011, pp. 288 –291.

[5] T. G. Leong, A. M. Zarafshar, and D. H. Gracias, "Three-dimensional fabrication at small size scales," *Small*, vol. 6, no. 7, pp. 792–806, 2010. [Online]. Available: http://dx.doi.org/10.1002/smll.200901704

[6] M. Piñeirua, J. Bico, and B. Roman, "Capillary origami controlled by an electric field," Apr. 2010.

[7] Z. Wang, F.-C. Wang, and Y.-P. Zhao, "Tap dance of a water droplet," *Royal Society of London Proceedings Series A*, vol. 468, pp. 2485–2495, Sep. 2012.

[8] H. Cho, H.-Y. Kim, J. Y. Kang, and T. S. Kim, "How the capillary burst microvalve works," *Journal of Colloid and Interface Science*, vol. 306, no. 2, pp. 379 – 385, 2007. [Online]. Available: http://www.sciencedirect.com/science/article/pii/S0021979706009969